Excitation energy dependence of prompt fission γ-ray emission from ^{241}Pu*

D. Gjestvang [1,*] S. Siem,[1,†] F. Zeiser [1] J. Randrup,[2] R. Vogt,[3,4] J. N. Wilson,[5] F. Bello-Garrote [1] L. A. Bernstein,[2,6]
D. L. Bleuel [3] M. Guttormsen [1] A. Görgen [1] A. C. Larsen,[1] K. L. Malatji [7,8] E. F. Matthews,[6] A. Oberstedt,[9]
S. Oberstedt,[10] T. Tornyi,[11] G. M. Tveten [1,‡] and A. S. Voyles[6]

[1]*Department of Physics, University of Oslo, N-0316 Oslo, Norway*
[2]*Nuclear Science Division, Lawrence Berkeley National Laboratory, Berkeley, California 94720, USA*
[3]*Nuclear and Chemical Sciences Division, Lawrence Livermore National Laboratory, Livermore, California 94551, USA*
[4]*Physics and Astronomy Department, University of California, Davis, California 95616, USA*
[5]*Université Paris-Saclay, CNRS/IN2P3, IJCLab, 91405 Orsay, France*
[6]*Nuclear Engineering Department, University of California, Berkeley, California 94720, USA*
[7]*Department of Subatomic Physics, iThemba LABS, P.O. Box 722, Somerset West 7129, South Africa*
[8]*Physics Department, Stellenbosch University, Matieland 7602, South Africa*
[9]*Extreme Light Infrastructure-Nuclear Physics (ELI-NP), Horia Hulubei National Institute for Physics and Nuclear Engineering (IFIN-HH),
077125 Bucharest-Magurele, Romania*
[10]*European Commission, Joint Research Centre, Directorate G for Nuclear Safety and Security, Unit G.2, 2440 Geel, Belgium*
[11]*Institute for Nuclear Research (Atomki), 4026 Debrecen, Hungary*

Prompt fission γ rays (PFGs) resulting from the ^{240}Pu$(d,p$f$)$ reaction have been measured as a function of fissioning nucleus excitation energy E_x at the Oslo Cyclotron Laboratory. We study the average total PFG multiplicity per fission, the average total PFG energy released per fission, and the average PFG energy. No significant changes in these characteristics are observed over the range $5.75 < E_x < 8.25$ MeV. The physical implications of this result are discussed. The experimental results are compared to simulations conducted using the computational fission model FREYA. We find that FREYA reproduces the experimental PFG characteristics within 8% deviation across the E_x range studied. Previous excitation energy-dependent PFG measurements conducted below the second-chance fission threshold have large uncertainties, but are generally in agreement with our results within a 2σ confidence interval. However, both a published parametrization of the PFG energy dependence and the most recent PFG evaluation included in ENDF/B-VIII.0 were found to poorly describe the PFG excitation-energy dependence observed in this and previous experiments.

I. INTRODUCTION

Eighty years have passed since the discovery of nuclear fission [1,2] and yet important aspects of fission remain to be understood. Computational models aiming to describe fission rely on experimental data to benchmark their calculations. Therefore, precision measurements of fission fragments, neutrons, and γ rays, and the correlations between them, are vital to test the current understanding of how fission proceeds.

Following the revived interest in fission, originating from its role in the nucleosynthesis of heavy elements [3] and the development of Generation-IV reactor concepts [4], studies are broadened to include hitherto unexplored details of nuclear fission. Prompt fission γ rays (PFGs), emitted in the final stages of fragment deexcitation, were first measured in the 1970s for selected actinides [5,6] and were found to carry only

a small fraction of the total energy release. They were thus long considered to be of little importance for understanding the fission process. However, PFGs carry the majority of the angular momentum generated in fission [7] and are therefore essential for understanding the state of the fragments just after scission. Furthermore, PFGs can deposit energy far away from where they are emitted, creating potential heating challenges in nuclear reactors [4]. Therefore, experiments measuring PFG characteristics for new fissioning systems and energy regions have been conducted [8–10], and progress has been made in accurate modeling PFG emission [11–14].

A key question, essential for reactor applications and basic fundamental physics, is how the prompt γ-ray emission in fission is affected when the excitation energy E_x of the fissioning system increases. Currently, only limited experimental data exist where the PFGs have been extracted for more than one E_x [8,15–19]. Here we present measurements of the PFG characteristics from the ^{240}Pu$(d,p$f$)$ reaction, extracted over a range of ^{241}Pu* excitation energies. The characteristics investigated are the average total γ-ray energy emitted per fission, $\overline{E}_{\gamma,\mathrm{tot}}$, average total γ-ray multiplicity per fis-

*dorthea.gjestvang@fys.uio.no
†sunniva.siem@fys.uio.no
‡Present address: Expert Analytics AS, N-0160 Oslo, Norway.
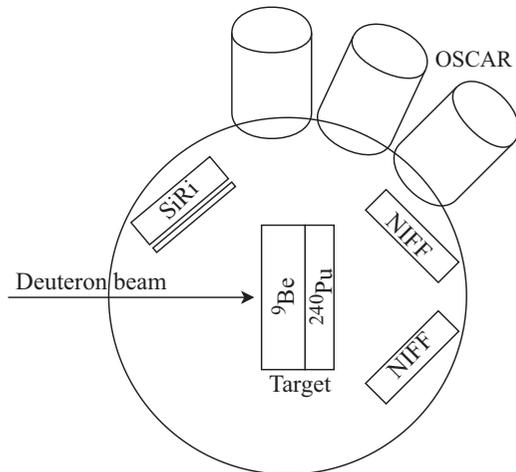
FIG. 1. Experimental setup for detecting PFGs from the ^{240}Pu(d,pf) reaction. Although only three LaBr$_3$ detectors are depicted, 28 were used in the experiment. Two of the four NIFF counters are illustrated. The figure is not to scale.

FIG. 2. Fission-gated spectrum showing the time difference Δt_{LaBr_3} between a proton in the ΔE detector and γ rays in OSCAR, plotted against the γ-ray energy detected by the LaBr$_3$. The time gates used to distinguish PFGs from PFNs via ToF are shown in black.

sion, $\overline{M}_\gamma$, and average γ-ray energy, $\overline{\varepsilon}_\gamma$. By studying how these quantities change with E_x, we investigate how increased excitation energy impacts γ-ray emission from the fission fragments. Furthermore, the measurements are compared to predictions made by the fission model FREYA (Fission Reaction Event Yield Algorithm), which simulates fission events where energy as well as linear and angular momentum are conserved [20]. This comparison between simulation and experiment is a benchmark of the current understanding of γ-ray emission in fission, and is expected to provide new insight into the fission process [21].

II. EXPERIMENT AND DATA ANALYSIS

The experiment presented in this paper was performed in April 2018 at the Oslo Cyclotron Laboratory (OCL). The experimental setup is illustrated in Fig. 1. A target of $\approx$0.4 mg/cm^2 thick ^{240}Pu on a fronting of 2.3 mg/cm^2 ^{9}Be, produced as described in Ref. [22], was bombarded with a beam of 13.5 MeV deuterons. The outgoing protons from the (d,pf) reaction were detected by SiRi, a silicon ΔE-E detector consisting of eight 1550 μm thick E pads each fronted with eight 130 μm thick ΔE strips [23]. SiRi was placed 5 cm away from the target, covering the angles $126°$–$140°$ with respect to the beam axis. By analyzing the energy and emission angle of the outgoing protons, the excitation energy of the compound nuclei (CN) ^{241}Pu* could be reconstructed [24].

To distinguish fission events from other reaction channels, fission fragments were detected using NIFF (Nuclear Instrument for Fission Fragments), consisting of four parallel plate avalanche counters (PPACs) [25]. NIFF is assembled in a lamp-shade geometry where each counter is placed at an angle of $45°$ with respect to the beam axis. The distance from the detector to the center of the target is about 5 cm, and an aperture in the center allows the beam to pass through. NIFF does not give a signal for light ejectiles such as ^{4}He and has
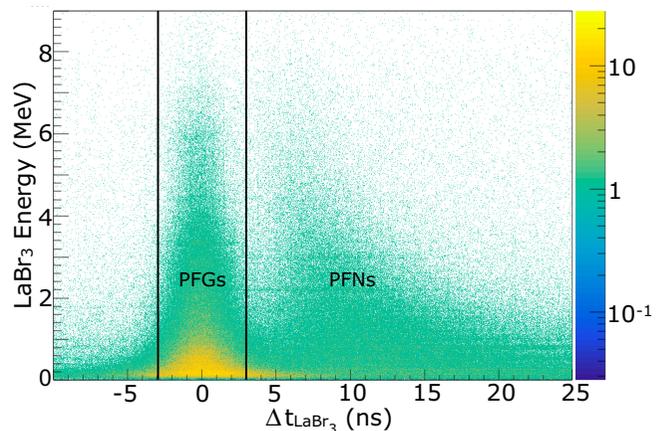
no mass resolution, but provides high efficiency as only one of the fragments needs to be detected to tag a fission event.

The reaction chamber, containing the target, SiRi, and NIFF, was surrounded by the Oslo Scintillator Array (OSCAR). OSCAR consists of 30 new LaBr$_3$:Ce scintillator detectors used for photon detection. Each detector crystal is cylindrical and measures 3.5 in$\times$ 8 in (diameter $\times$ length) [26]. In this experiment, 28 of the 30 detectors were operational. LaBr$_3$ detectors are known for balancing good energy resolution with a fast decay time and are therefore well suited for coincidence experiments like PFG measurements. In the experiment, 27 of OSCAR's detectors were situated at a 20 cm distance from the target, while one was pulled back to 40 cm. The present work is the first use of OSCAR for PFG detection.

In this experiment, the data acquisition system was set to capture all events where the fission fragments and γ rays arrived within a $\pm$1.5 μs time interval relative to the detection of a proton. Details of the data acquisition will follow in Ref. [27]. In order to extract prompt fission γ rays, coincidence between a proton, a fission fragment, and a γ ray was required. These events are obtained by applying prompt time gates in the time-of-flight (ToF) spectrum. The fission-gated ToF spectrum for detected LaBr$_3$ energies is shown in Fig. 2, where Δt_{LaBr_3} is the time difference between the arrival of a proton in the ΔE detector and the arrival of a γ ray in OSCAR. Here the flight time of the proton has been corrected for, ensuring that the peak in Fig. 2 is centered around zero for both high- and low-energy proton events. The FWHM time resolution of the experiment was $\approx$3 ns. To separate the PFGs from the prompt fission neutrons (PFNs), which produce signals resembling γ rays in the LaBr$_3$ detectors, a time gate of $\pm$3 ns was chosen. This was a compromise between maximizing statistics and minimizing the PFN contribution. With this $\pm$3 ns time gate and 20 cm distance from the target to the detector, the majority of the neutrons below 10 MeV could be rejected.
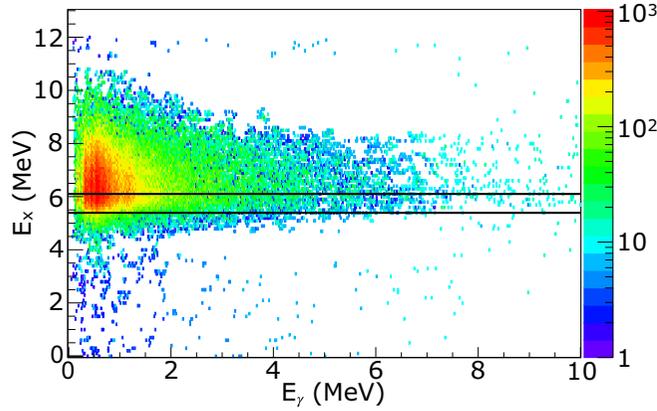
FIG. 3. Unfolded, background-subtracted coincidence matrix, showing the energies E_γ of γ rays from $(d, pf\gamma)$ events as a function of ^{241}Pu* excitation energy E_x. The values of the inner and outer fission barriers, 6.14 ± 0.5 MeV and 5.4 ± 0.5 MeV, respectively [32], are drawn in black.

Similarly, a time gate on Δt_{NIFF} of ± 4.6 ns was used to select prompt fission fragments, where Δt_{NIFF} is the time difference between the arrival of a proton in the ΔE detector and the arrival of a fission fragment in NIFF. Here, the same relative width between the prompt time cut and the time resolution of the fission detectors were used as for the γ-ray detectors. As the NIFF time resolution was worse than the LaBr$_3$, the time scale of the events are best described by Δt_{LaBr_3}.

The γ-ray response of OSCAR [28,29] was corrected for by applying the unfolding procedure described in Ref. [30]. This procedure has recently been further developed and now propagates the statistical uncertainties throughout the unfolding routine [31]. The unfolded, background-subtracted coincidence matrix showing the detected γ-ray energies E_γ for different ^{241}Pu* excitation energies E_x is shown in Fig. 3.

A. Verification using ^{252}Cf

The prompt fission γ-ray characteristics from the spontaneous fission of ^{252}Cf are well known and thus measurements of these serve as a benchmark for our PFG extraction routine.

FIG. 4. Extracted prompt fission γ-ray spectrum for ^{252}Cf, compared to the previous measurements of Verbinski et al. [33], Billnert et al. [34], and Oberstedt et al. [35] (marked Q489). The latter two measurements were conducted using LaBr$_3$ detectors. (b) shows the same data as (a) magnified to highlight the low-energy region. The uncertainties on the spectrum in this work are statistical. The deviation at low energies can be explained by the difference in relative time gates, see text.

We measured PFGs emitted from a ^{252}Cf source, the activity of which was measured to 3.3 kBq in April 2012, using the same experimental setup as described in Sec. II. In Fig. 4, the PFG spectrum from ^{252}Cf(sf) measured in this work is compared to previous measurements [33–35]. There is good agreement for γ-ray energies above ≈ 0.5 MeV and the structures in the spectrum below ≈ 0.5 MeV also match those of earlier measurements. For $E_\gamma < 0.5$ MeV, we note that there is a depletion in the measured γ-ray multiplicity relative to the earlier measurements, which is reflected in the calculated PFG characteristics presented in Table I. Figure 2 shows that this depletion arises from low-energy γ rays that fall outside

TABLE I. PFG characteristics determined from previous ^{252}Cf(sf) experiments using LaBr$_3$ detectors, compared to uncorrected and corrected values from the present work. The uncertainties on the uncorrected values are statistical, propagated through the γ-ray unfolding routine. The scaling factors used to obtain the corrected values are also given. In Ref. [35], three separate measurements were conducted using LaBr$_3$ detectors, marked Q489, Q491, and 2987, respectively.

Reference	$\overline{M}_\gamma$	$\overline{E}_{\gamma,tot}$ [MeV]
This work, uncorrected	6.37 ± 0.03	6.18 ± 0.05
This work, corrected	8.28 ± 0.04 [a]	6.61 ± 0.05 [b]
Scaling factors	1.30	1.07
Billnert et al. [34]	8.30 ± 0.08	6.64 ± 0.08
Oberstedt et al. [35] (Q489)	8.29 ± 0.07	6.74 ± 0.09
Oberstedt et al. [35] (Q491)	8.28 ± 0.08	6.76 ± 0.09
Oberstedt et al. [35] (2987)	8.28 ± 0.07	6.51 ± 0.07

[a]The uncertainty listed is the propagated statistical uncertainty.
[b]See footnote a.

of the ± 3 ns time gate, a narrower gate relative to the time resolution than those used in Refs. [33–35]. As described above, a wider time gate could not be used in the present experiment due to contamination of PFNs. By comparing our measured ^{252}Cf(sf) PFG characteristics to those obtained by selected previous experiments (see Table I) chosen because they also use LaBr$_3$ γ-ray detectors, we estimate that about 10% of the γ-ray energy and 20% of the multiplicity are excluded due to the narrow prompt time gate. The effect of the time gate on the observed value of M_γ has recently been thoroughly discussed in Ref. [36].

In this paper, we study the E_x dependence of PFG emission from ^{241}Pu*. Because Fig. 4(a) shows that the PFG spectrum for ^{252}Cf is reproduced for $E_\gamma \gtrsim 0.5$ MeV, we will be sensitive to potential changes E_x in the spectrum of ^{241}Pu* above this γ-ray energy. Furthermore, it is reasonable to assume that the same percentage of the PFGs are lost in the ^{240}Pu(d, pf) measurement as for ^{252}Cf(sf). Therefore, significant changes in the ^{241}Pu* PFG spectrum below ≈ 0.5 MeV are expected to be observed as well.

In order to facilitate comparison to previous experiments despite the difference in time gates, we introduce a scaling procedure for $\overline{E}_{\gamma,\text{tot}}$ and $\overline{M}_\gamma$. Here, the previous ^{252}Cf(sf) measurements are used to find the scaling parameters needed to correct the multiplicity and total energy. The scaling parameters are taken as the constant ratio between, e.g., the multiplicity found in this work and the uncertainty-weighted average $\overline{M}_\gamma$ reported by the previous studies. The scaling parameters and the corrected ^{252}Cf(sf) PFG characteristics are found in Table I. The same scaling parameters are later applied to the extracted ^{241}Pu PFG multiplicity and total energy, and from these the scaled $\overline{\varepsilon}_\gamma = \overline{E}_{\gamma,\text{tot}}/\overline{M}_\gamma$ is determined.

B. FREYA simulation

The computational fission model FREYA version 2.0.3 was used to simulate the prompt fission γ rays resulting from the fission of ^{241}Pu*. In FREYA only a selected number of fissioning nuclei are included, and the fission of ^{241}Pu* is currently not among them. To implement this isotope, the fission fragment mass distribution $Y(A)$ and the total kinetic energy of the fragments TKE(A) were needed, neither of which were available from experiments. They were therefore obtained from the fission model GEF (GEneral description of Fission observables) [14]. TKE(A) and $Y(A)$ are known to change with the excitation energy of the compound nucleus, thus their energy dependencies had to be determined in order to simulate energy-dependent fission in FREYA. A five-parameter-Gaussian fit was used to parametrize $Y(A, E_x)$. TKE(A, E_x) was determined by shifting TKE(A_H) to match the evaluated PFN multiplicity for each E_x, where A_H is the mass of the heavy fragment. Further details of this procedure are found in Ref. [37]. As FREYA only simulates neutron-induced and spontaneous fission, the ^{240}Pu(d, pf) reaction was mimicked by the (n,f) surrogate reaction, see Sec. IV for further discussion regarding potential differences between the two reactions. By using the reaction ^{240}Pu(n,f) one obtain fissions of ^{241}Pu* with excitation energy $E_x = E_n + S_n$. Here S_n is the neutron separation energy of ^{241}Pu. As ^{240}Pu is not

fissile, the E_x equivalent of thermal neutron-induced fission, $E_n \approx 0$ MeV, lies below the double-humped fission barrier, whose values are 6.14 ± 0.5 MeV and 5.4 ± 0.5 MeV for the inner and outer barrier, respectively [32].

A brief summary of how FREYA treats γ-ray emission is given below; a full account is found elsewhere [11,20]. Neutrons are evaporated until no longer energetically possible, which is when the excitation energy of the fragment falls below S_n, and thus γ-ray emission begins. First, statistical γ rays are sampled from a black-body spectrum, each carrying $1\hbar$ of the fragment's angular momentum. After reaching the yrast line, rotational $E2$ γ rays are emitted to exhaust the remaining excitation energy and angular momentum. Whenever available for the fragment in question, FREYA will use the evaluated discrete transitions from the RIPL-3 library [38] instead of the statistical and collective sampling.

The two FREYA input parameters $t_{\max}$ and $g_{\min}$ were considered in this work, as FREYA does not simulate photons emitted from states with half-lives longer than $t_{\max}$ or with energies lower than $g_{\min}$. In accordance with the experimental prompt time cut, $t_{\max}$ was chosen to be 3 ns. The value of $g_{\min}$ reflects the energy threshold of γ rays included in the analysis and was chosen to be 0.1 MeV, as used in previous experiments [10,16,35].

The ^{240}Pu(n,f) reaction was simulated for E_n in the range 0.0–5.0 MeV with steps of 0.5 MeV, which corresponds to the ^{241}Pu* excitation energy range 5.2–10.2 MeV. We ran 10^6 fission events per energy.

III. RESULTS

Figure 3 shows that the majority of the $(d, pf\gamma)$ events arrive when the excitation energy of ^{241}Pu* exceeds ≈ 5.5 MeV, and thus the onset of fission corresponds well to the values of the double-humped fission barrier reported in Ref. [32]. The prompt fission γ rays were extracted from the unfolded coincidence matrix for the ^{241}Pu excitation energy range from 5.5–8.5 MeV using E_x bins of 0.5 MeV. Outside this region few fissions are registered and spectrum is dominated by the background of random coincidences with γ rays from ^{9}Be. As stated above, the γ-ray threshold was set to 0.1 MeV in the analysis. The upper energy limit chosen in PFG studies is usually in the range 6–10 MeV and has little impact on the PFG characteristics [39]. We thus study the PFGs in the range from 0.1–10 MeV, as no γ rays with higher energy were observed.

The PFG spectra for different E_x bins is shown in Fig. 5. Note that these spectra have not been subject to the corrections described in Sec. II A. The uncertainties included for the experimental spectra are the statistical uncertainties, propagated through the γ-ray unfolding routine, as well as the statistical uncertainty on the number of fissions detected. For clarity, uncertainties are only shown for one spectrum.

To further understand the PFG behavior with E_x, the PFG characteristics were calculated from Fig. 5. The resulting values for $\overline{M}_\gamma$, $\overline{E}_{\gamma,\text{tot}}$, and $\overline{\varepsilon}_\gamma$ as a function of E_x are shown in Fig. 6. The data are shown both before and after the correction procedure described in Sec. II A was applied. We emphasize that the sole effect of this correction is a scaling of all the
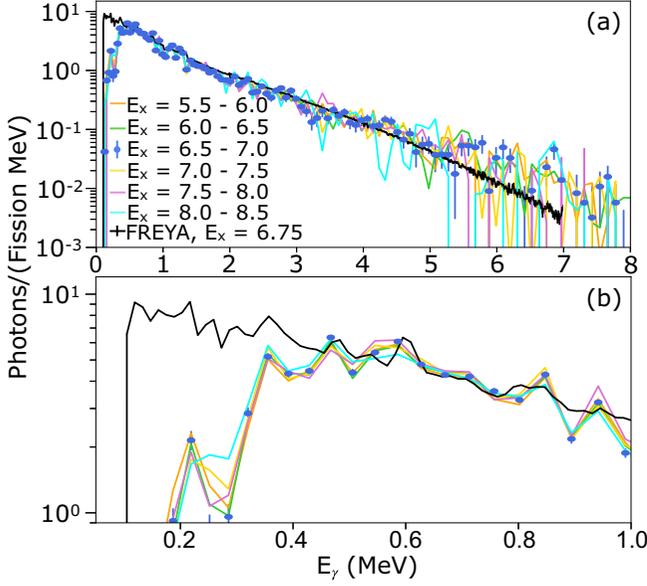
FIG. 5. Extracted, uncorrected prompt fission γ-ray spectra for ^{241}Pu for excitation energies in the range 5.5–8.5 MeV, compared to the FREYA prediction at $E_x = 6.75$ MeV. Statistical uncertainties are shown for the experimental spectrum in the excitation energy bin 6.5–7.0 MeV to increase readability. The statistical uncertainties on the FREYA spectrum are smaller than the marker size for lower energies. (b) shows the same data as in (a), magnified to highlight the low-energy region. We observe that the experimental spectra for different E_x are similar.

PFG characteristics, included to facilitate comparison to the FREYA simulations and previous studies of other fissioning systems.

In order to quantify the rate of change observed in the PFG characteristics, we introduce the relative change of the PFG

FIG. 6. Evolution of (a) $\overline{M}_\gamma$, (b) $\overline{E}_{\gamma,\text{tot}}$, and (c) $\overline{\varepsilon}_\gamma$ with ^{241}Pu* excitation energy. The full red, blue, and green lines show the weighted linear interpolation of the uncorrected and corrected experimental data, and the FREYA results, respectively. The statistical uncertainties on the FREYA values are negligible. The uncertainties on the corrected values are the propagated statistical uncertainties. The uncertainty on $\overline{\varepsilon}_\gamma$ is calculated by assuming the uncertainties on $\overline{M}_\gamma$ and $\overline{E}_{\gamma,\text{tot}}$ are independent.

characteristics with excitation energy, the slopes of $\overline{M}_\gamma$, $\overline{E}_{\gamma,\text{tot}}$, and $\overline{\varepsilon}_\gamma$ with increasing E_x; $\Delta\overline{M}_\gamma/\Delta E_x$, $\Delta\overline{E}_{\gamma,\text{tot}}/\Delta E_x$, and $\Delta\overline{\varepsilon}_\gamma/\Delta E_x$. This introduction is justified by the observation in Fig. 6 that the PFG characteristics are to first order linear in E_x below the threshold of second-chance fission, which is supported by previous work [8]. The interpretation of, e.g., $\Delta\overline{M}_\gamma/\Delta E_x$ is how many extra γ rays are emitted per MeV increase in E_x of the fissioning nucleus.

TABLE II. PFG measurements and predictions of the PFG dependence on E_x below the threshold of second-chance fission. Where two energies were used, these are given as E_1, E_2, otherwise the energy range is given. In the case of Laborie *et al.* [15], only the two lowest incoming neutron energies are used to stay below the threshold of second-chance fission. This threshold is found by adding the S_n of the compound nucleus A from Ref. [40] and to the energy of the lower fission barrier of the (A-1) daughter nucleus [32].

Reference	Reaction	E_n [MeV]	E_x [MeV]	$\Delta\overline{M}_\gamma/\Delta E_x$ [MeV^{-1}]	$\Delta\overline{E}_{\gamma,\text{tot}}/\Delta E_x$	$\Delta\overline{\varepsilon}_\gamma/\Delta E_x$
This work, experiment	^{240}Pu(d,pf)	–	5.75–8.25	0.06 ± 0.02	0.01 ± 0.05	-0.01 ± 0.01
This work, experiment, corrected	^{240}Pu(d,pf)	–	5.75–8.25	0.08 ± 0.03	0.01 ± 0.06	-0.01 ± 0.01
This work, FREYA-2.0.3	^{240}Pu($n,$f)	0.00–5.00	5.24–10.24	0.06	0.07	0.00
Previous experiments:						
Fréhaut *et al.* [19] (1983)	^{235}U($n,$f)	1.15–5.42	7.69–11.97	N/A	0.14 ± 0.01	N/A
Rose *et al.* [8] (2017)	^{239}Pu(d,pf)	–	4.81–8.49	0.23 ± 0.20	0.27 ± 0.07	0.00 ± 0.03
Rose *et al.* [8] (2017)	^{233}U(d,pf)	–	5.12–9.68	0.12 ± 0.23	0.13 ± 0.10	0.00 ± 0.03
Laborie *et al.* [15] (2018)	^{238}U($n,$f)	1.60, 5.10	6.41, 9.91	0.05 ± 0.27	-0.06 ± 0.25	-0.02 ± 0.01
Qi *et al.* [16] LaBr$_3$ (2018)	^{238}U($n,$f)	1.90, 4.80	6.71, 9.61	0.34 ± 0.18	0.39 ± 0.25	0.01 ± 0.04
Qi *et al.* [16] PARIS (2018)	^{238}U($n,$f)	1.90, 4.80	6.71, 9.61	0.19 ± 0.16	0.24 ± 0.22	0.01 ± 0.04
Predictions/Evaluations:						
Oberstedt *et al.* [41] (2017)[a]	^{240}Pu($n,$f)	0.00–5.00	5.24–10.24	0.42 ± 0.03	0.13 ± 0.08	-0.02 ± 0.01
ENDF-B/VIII.0, Stetcu *et al.* [42] (2020)	^{239}Pu($n,$f)	0.00–5.00	6.53–11.53	0.51 ± 0.09	0.43 ± 0.07	0.00 ± 0.00

[a]The systematics for predicting PFG characteristics presented in Ref. [41] are applied to the ^{240}Pu($n,$f) reaction, where the necessary input data were taken from the ENDF/B-VIII.0 evaluation.

The PFG properties show little change with increasing E_x, a feature that is evident when studying the extracted values for $\overline{M}_\gamma$, $\overline{E}_{\gamma,\text{tot}}$, and $\overline{\varepsilon}_\gamma$ in Fig. 6. This is reflected in the relative changes: weighted linear interpolation gives $\Delta \overline{M}_\gamma / \Delta E_x = 0.07 \pm 0.03$ MeV^{-1}, $\Delta \overline{E}_{\gamma,\text{tot}} / \Delta E_x = 0.01 \pm 0.05$, and $\Delta \overline{\varepsilon}_\gamma / \Delta E_x = -0.01 \pm 0.01$ for the uncorrected PFG characteristics. The impact of the correction on the relative changes is minimal (see Table II), and thus the use of this scaling procedure has no impact on the conclusions of the paper.

IV. DISCUSSION

A. Experiment and FREYA

The present experiment is the first measurement of prompt fission γ rays from ^{241}Pu* and direct comparisons of the PFG characteristics to previous experiments are therefore not possible. Typical values for $\overline{M}_\gamma$ and $\overline{E}_{\gamma,\text{tot}}$ across different fissioning systems are in the range of 6.5–8 and 5–7 MeV, respectively [9,10]. We see from Fig. 5 that the corrected PFG characteristics for ^{241}Pu* are within these expected intervals.

When comparing the FREYA γ-ray spectrum for $E_x = 6.75$ MeV to the experimental spectrum for the excitation energy bin $E_x = 6.5 - 7.0$ MeV in Fig. 5, we see that the calculated spectrum is very similar to the measured one for $E_\gamma \gtrsim 0.5$ MeV. As discussed in Sec. II A, the discrepancies for $E_\gamma \lesssim 0.5$ MeV were expected. Figure 5(a) shows that FREYA reproduces the shapes of the γ-ray spectrum quite well for $E_\gamma \lesssim 0.5$ as well, probably due to the inclusion of discrete nuclear transitions from the RIPL-3 library in the γ-ray decay procedure. Figure 5 indicates that FREYA might underestimate the photon yield for $E_\gamma \gtrsim 5.5$ MeV, where structures seem to be present in the experimental spectra. Such structures in the high-energy tail of the PFG spectrum have previously been observed experimentally and are believed to originate from nuclear shell effects in the fission fragments [43]. Nevertheless, deviations at higher energies do not significantly affect the calculated values for the PFG characteristics due to the exponentially falling nature of the spectrum.

The similarity between the FREYA γ-ray spectra and the experimental spectra in Fig. 5(a) is reflected in the integrated characteristics shown in Fig. 6. The simulated values of $\overline{E}_{\gamma,\text{tot}}$, presented in Fig. 6(b) lie within a 2σ interval across the excitation energy range studied. Furthermore, $\overline{M}_\gamma$ and $\overline{\varepsilon}_\gamma$ in Figs. 6(a) and 6(c) calculated by FREYA are within 8% of the corrected experimental values, though the calculated γ-ray multiplicity and average γ-ray energy are, respectively, higher and lower than the corrected experimental results. This deviation in the absolute characteristics might be a result of either the simple correction procedure presented in Sec. II A not being sufficiently precise or that FREYA simulates an excess of low-energy γ rays.

A striking feature of Fig. 6 is the apparent excitation energy independence of the observed PFG characteristics, reflected in Table II where the slopes of these quantities are found to be small. Only the value of $\Delta \overline{M}_\gamma / \Delta E_x$ is statistically significant in a 2σ confidence interval. This indicates that when

additional E_x is supplied to the fissioning nucleus and hence to the fragments, only a small or even negligible fraction of the extra energy is released as emission of prompt γ rays.

The trend observed in Fig. 6 of small increase in the PFG characteristics with E_x is supported by FREYA as seen by the values for the relative changes in Table II, where the FREYA simulated for $\Delta \overline{M}_\gamma / \Delta E_x$, and $\Delta \overline{E}_{\gamma,\text{tot}} / \Delta E_x$ are within a 1σ deviation from the experimental values. This overall agreement between the simulated and experimental relative changes indicate that the deexcitation model employed by FREYA captures the main mechanisms of excitation energy-dependent PFG emission. We note that the FREYA calculated $\Delta \overline{M}_\gamma / \Delta E_x$ and $\Delta \overline{E}_{\gamma,\text{tot}} / \Delta E_x$ are weakly energy dependent, but as they change in parallel with each other, $\Delta \overline{\varepsilon}_\gamma / \Delta E_x$ is zero over this excitation energy range.

Understanding the behavior of the γ-ray emission simulated by FREYA gives insights into the physical mechanisms behind the experimentally determined slopes. As described above, $Y(A)$ is energy dependent and becomes progressively more symmetric with increasing E_n [37] and thus equivalently E_x. As $Y(A)$ changes, the weighted average of each γ-emitting fragment also changes, indirectly affecting PFG emission. However, the change of $Y(A)$ is expected to be small over the excitation energy interval studied. Furthermore, the PFN multiplicity is known to increase with higher E_x. The fission fragments are thus less neutron-rich at the onset of γ-ray emission, yielding a larger average S_n among the fragments. Because S_n is effectively the upper limit for γ-ray emission in FREYA, this might explain an increase in $\overline{E}_{\gamma,\text{tot}}$ with E_x. Changes in the average S_n of the fragments have previously been linked to differences in the PFG characteristics [10].

Both of the aforementioned mechanisms could be sources of the dependences of the PFG characteristics on E_x. A glance at the trends in both the measured and simulated characteristics in Fig. 6 shows that these effects are small or even negligible, with only $\leqslant 0.07$ extra γ rays carrying $\leqslant 80$ keV more energy being emitted per MeV increase in E_x.

As we observe only a small fraction of the added extra energy results in γ-ray emission, this raises the question where the energy is distributed. Energy sharing in fission is a intricate and poorly understood process, as each fragment emerges both with kinetic and excitation energy. More neutrons are known to be emitted with increasing E_x, which implies that the neutrons carry away a portion of the added E_x. It thus seems that the fragment prefers to emit another neutron if possible, rather than an additional γ ray.

We note that though we make direct comparison between ^{240}Pu(*n*,f) as simulated by FREYA and the experimental surrogate reaction ^{240}Pu(*d*,*p*f), these reactions may not populate the same states in the compound nuclei. The charged-particle reaction is expected to induce more angular momentum in the fissioning nucleus, and the PFGs are known to exhaust most of the angular momentum of the fragments. It is not clear how the angular momentum of the initial compound nucleus which fissions is related to those of the resulting fission fragments. An experiment comparing the impact of using the (*d*,*p*f) versus (*n*,f) found a significant difference in the PFG characteristics [8], though this might be because of PFN

contamination. On the other hand, recent theoretical work suggests that the angular momentum of the compound system does not significantly influence the fragment spins [44]. This question of angular momentum propagation in fission will be further investigated in upcoming experiments at the OCL.

B. Previous experiments

As mentioned above, there are few experiments in the literature where the PFGs are extracted as a function of CN excitation energy. Nevertheless, a handful of measurements comparing thermal and fast neutron-induced fission have been conducted recently to provide vital information for the construction of the Generation-IV fast reactors [8,15–18]. This enables us to extract their values of $\Delta \overline{M}_\gamma / \Delta E_x$, $\Delta \overline{E}_{\gamma,\text{tot}} / \Delta E_x$, and $\Delta \overline{\varepsilon}_\gamma / \Delta E_x$ by fitting a linear slope to their results below the threshold for second-chance fission. Though the fissioning nuclei are not the same in the different experiments, we expect the mechanism for the energy sharing in fission and thus the energy dependence of the PFGs from different fissioning isotopes to be largely the same.

The deduced values for the relative changes of recent PFG measurements are presented in Table II. We have limited this table to only include experiments where the same setup was used for measurements at different E_x and where E_x is below the threshold for second-chance fission. The latter is to simplify interpretation because the fissioning nucleus is the same across the whole energy range considered.

From the extracted values of $\Delta \overline{M}_\gamma / \Delta E_x$, $\Delta \overline{E}_{\gamma,\text{tot}} / \Delta E_x$, and $\Delta \overline{\varepsilon}_\gamma / \Delta E_x$ we see that per additional MeV of excitation energy in the compound system, the previous measurements observed 0.05–0.34 more γ rays per fission, carrying 0.13–0.39 MeV extra energy. The average photon energy $\overline{\varepsilon}_\gamma$ is observed to be approximately constant. Due to the large uncertainties, the majority of the slopes are consistent with zero to a 2σ confidence level.

We see that both $\Delta \overline{M}_\gamma / \Delta E_x$ and $\Delta \overline{E}_{\gamma,\text{tot}} / \Delta E_x$ from previous experiments are generally larger compared to the ones obtained from the current experiment. A possible reason for this is that some of the previous experiments measured PFGs solely at two different values of E_x below the second-chance fission threshold, and all the measurements have significant uncertainties. Consequently, the slopes are correspondingly uncertain. Additionally, a deviation could originate from a difference in the population of isomeric states. If more isomeric states are populated with increasing excitation energy, fewer γ rays might be captured in the prompt time gate, thus impacting $\Delta \overline{M}_\gamma / \Delta E_x$, and $\Delta \overline{E}_{\gamma,\text{tot}} / \Delta E_x$.

Despite these possible differences, we see from Table II that the previous experiments largely agree with the values of $\Delta \overline{M}_\gamma / \Delta E_x$ and $\Delta \overline{E}_{\gamma,\text{tot}} / \Delta E_x$ found for ^{240}Pu(d, pf) within a 2σ interval. The measurements by Qi et al. and Laborie et al. report large uncertainties, and the former give higher values for the relative change parameters. The weighted average slopes among the previous experiments are 0.21 MeV^{-1} and 0.22 for $\Delta \overline{M}_\gamma / \Delta E_x$ and $\Delta \overline{E}_{\gamma,\text{tot}} / \Delta E_x$ respectively, where the measurement by Fréhaut et al. in Ref. [19] has been omitted due to a seemingly underestimated uncertainty on the slope.

C. Previous estimations of PFG dependence on E_x

Two previous works attempted to estimate the dependence on prompt fission γ-ray emission on E_x for different fissioning systems. In Ref. [41], Oberstedt et al. introduced an empirical parametrization to predict the PFG characteristics based on the mass and charge of the fissioning nucleus. In order to include the unknown E_x dependence of the PFGs, they assume that there is a direct relationship between the γ-ray and neutron multiplicities. Furthermore, in Ref. [42] Stetcu et al. recently evaluated available experimental data to recommend how the PFG characteristics are expected to change with inceased E_x.

Again, we find the values of $\Delta \overline{M}_\gamma / \Delta E_x$ and $\Delta \overline{E}_{\gamma,\text{tot}} / \Delta E_x$ below the threshold for second-chance fission from from the evaluations presented by Oberstedt et al. and Stetcu et al. These are presented in Table II. Here we see that there is a significant gap between the parametrization and evaluation on one hand, and the experimental data on the other. The values of $\Delta \overline{M}_\gamma / \Delta E_x$ from Refs. [41,42] are five times larger than those from the present experimental data, and more than twice as large as the average among previous experiments. Furthermore the value for $\Delta \overline{E}_{\gamma,\text{tot}} / \Delta E_x$ reported by Stetcu et al. is also noticeably larger than given by the experiments. The values for $\Delta \overline{\varepsilon}_\gamma / \Delta E_x$ from Oberstedt et al. and Stetcu et al. accurately reflect the available experimental data.

While there is a definitive lack of experimental data to which Refs. [41,42] can benchmark their suggested dependence on E_x, neither FREYA nor CGMF [45] (calculations from the latter are presented in Ref. [42]) support a marked increase in the PFG characteristics below the threshold for second-chance fission.

In light of these results, the assumption in Ref. [41] regarding the direct dependence of the γ-ray multiplicity on the energy-dependent neutron multiplicity should be revisited. Furthermore, the ENDF-B/VIII.0 evaluation by Stetcu et al. seems to put a large emphasis on PFG characteristics inferred from γ-ray production cross sections measured in the 1960s, which are ambiguous and inconsistent with other experimental results (see, for example, Fig. 9 in Ref. [42]). We also note that the results from Rose et al. [8] regarding the E_x dependence of the PFGs from the ^{239}Pu(d, pf) reaction seem to not be included in their evaluation of PFGs from ^{239}Pu(n,f).

As the PFG dependence on E_x is desirable information both for providing correct input for fast-reactor simulations and for reaching a deeper understanding of the mechanisms behind PFG emission, the observed deviations between the parametrization/evaluation, on one hand, and experiments/fission simulations, on the other, must be further investigated and resolved.

V. CONCLUSION AND OUTLOOK

Prompt fission γ-ray characteristics resulting from the fission of ^{241}Pu* have been measured in the excitation energy region 5.75–8.25 MeV. A verification measurement of the PFG spectrum from ^{252}Cf(sf) reproduces previous

measurements for $E_\gamma \gtrsim 0.5$ MeV, while for lower γ-ray energies there is a deviation. This is attributed to the narrow time gate necessary to reject PFNs by ToF. We will use a larger distance between the target and detector in upcoming experiments to further investigate this deviation. Employing the well-known ^{252}Cf(sf) PFG characteristics, correction factors were found and applied to the ^{241}Pu* PFG characteristics in order to facilitate comparison between different experiments. FREYA reproduces the corrected values of the average total γ-ray energy ($\overline{E}_{\gamma,\text{tot}}$) found in this work within a 2σ interval, and the average γ-ray multiplicity per fission ($\overline{M}_\gamma$) and average photon energy ($\overline{\varepsilon}_\gamma$) simulated by FREYA are within 8% of the experimental values across the excitation energy range studied.

To study the dependence of the PFG characteristics on E_x, new quantities that describe the energy dependence of the PFGs were extracted and analyzed. These were found to be small, with $\overline{M}_\gamma$, $\overline{E}_{\gamma,\text{tot}}$, and $\overline{\varepsilon}_\gamma$ all exhibiting little to no dependence on E_x below the threshold for second-chance fission. We observe smaller changes than seen in other previous experiments, though large experimental uncertainties reported in earlier work complicate the comparison. However, two separate evaluations of the PFG dependence on E_x yield significantly larger values for $\Delta\overline{M}_\gamma/\Delta E_x$ than the average among previous experiments. Therefore, more experiments must be conducted where PFGs are measured for different compound nucleus excitation energies. Such experiments are planned at the OCL and will hopefully bring a deeper understanding of the excitation energy partition in fission.

The data presented in Fig. 6 are available in Ref. [46].

[1] L. Meitner and O. R. Frisch, Disintegration of Uranium by neutrons: A new type of nuclear reaction, Nature (London) **143**, 239 (1939).

[2] O. Hahn and F. Strassmann, Über den Nachweis und das Verhalten der bei der Bestrahlung des Urans mittels Neutronen entstehenden Erdalkalimetalle, Sci. Nat. **27**, 11 (1939).

[3] S. Goriely, The fundamental role of fission during r-process nucleosynthesis in neutron star mergers, Eur. Phys. J. A **51**, 22 (2015).

[4] G. Rimpault, D. Bernard, D. Blanchet, C. Vaglio-Gaudard, S. Ravaux, and A. Santamarina, Needs of accurate prompt and delayed γ-spectrum and multiplicity for Nuclear Reactor Designs, Phys. Procedia **31**, 3 (2012).

[5] H. Nifenecker, C. Signarbieux, M. Ribrag, J. Poitou, and J. Matuszek, γ-neutron competition in the de-excitation mechanism of the fission fragments of ^{252}Cf, Nucl. Phys. A **189**, 285 (1972).

[6] F. Pleasonton, Fission of ^{233}U and ^{239}Pu, Nucl. Phys. A **213**, 413 (1973).

[7] A. Hotzel *et al.*, High-energy gamma-rays of 252Cf accompanying the spontaneous fission, Z. Phys. A **356**, 299 (1996).

[8] S. J. Rose *et al.*, Energy dependence of the prompt γ-ray emission from the (d, p)-induced fission of ^{234}U* and ^{240}Pu*, Phys. Rev. C **96**, 014601 (2017).

[9] S. Oberstedt, A. Oberstedt, A. Gatera, A. Göök, F.-J. Hambsch, A. Moens, G. Sibbens, D. Vanleeuw, and M. Vidali, Prompt fission γ-ray spectrum characteristics from ^{240}Pu(sf) and ^{242}Pu(sf), Phys. Rev. C **93**, 054603 (2016).

[10] L. Qi *et al.*, Potential of prompt γ-ray emission studies in fast-neutron induced fission: A first step, Eur. Phys. J. A **56**, 98 (2020).

[11] R. Vogt and J. Randrup, Improved modeling of photon observables with FREYA, Phys. Rev. C **96**, 064620 (2017).

[12] I. Stetcu, P. Talou, T. Kawano, and M. Jandel, Properties of prompt-fission γ rays, Phys. Rev. C **90**, 024617 (2014).

[13] M. J. Marcath, R. C. Haight, R. Vogt, M. Devlin, P. Talou, I. Stetcu, J. Randrup, P. F. Schuster, S. D. Clarke, and S. A. Pozzi, Measured and simulated ^{252}Cf(sf) prompt neutron-photon competition, Phys. Rev. C **97**, 044622 (2018).

[14] K. H. Schmidt, B. Jurado, C. Amouroux, and C. Schmitt, General description of fission observables: GEF model code, Nucl. Data Sheets **131**, 107 (2016).

[15] J.-M. Laborie, R. Billnert, G. Bélier, A. Oberstedt, S. Oberstedt, and J. Taieb, First experimental prompt gamma-ray spectra in fast-neutron-induced fission of ^{238}U, Phys. Rev. C **98**, 054604 (2018).

[16] L. Qi *et al.*, Statistical study of the prompt-fission γ-ray spectrum for ^{238}U(n, f) in the fast-neutron region, Phys. Rev. C **98**, 014612 (2018).

[17] A. Oberstedt, M. Lebois, S. Oberstedt, L. Qi, and J. N. Wilson, Prompt γ-ray characteristics from ^{235}U(n, f) at $\overline{E}_n = 1.7$ MeV, Eur. Phys. J. A **56**, 236 (2020).

[18] M. Lebois *et al.*, Comparative measurement of prompt fission γ-ray emission from fast-neutron-induced fission of ^{235}U and ^{238}U, Phys. Rev. C **92**, 034618 (2015).

[19] J. Fréhaut, A. Bertin, and R. Bois, Mesure de $\bar{\nu}_p$ et $\bar{E}_y$ Pour la Fission de ^{232}Th, ^{235}U et ^{237}Np Induite par des Neutrons D'Energie Comprise Entre 1 et 15 MeV, in *Nuclear Data for Science and Technology*, edited by K. H. Böckhoff (Springer, Dordrecht, 1983), pp. 78–81.

[20] J. M. Verbeke, J. Randrup, and R. Vogt, Fission reaction event yield algorithm FREYA 2.0.2, Comput. Phys. Commun. **222**, 263 (2018).

[21] L. A. Bernstein, D. A. Brown, A. J. Koning, B. T. Rearden, C. E. Romano, A. A. Sonzogni, A. S. Voyles, and W. Younes, Our future nuclear data needs, Annu. Rev. Nucl. Part. Sci. **69**, 109 (2019).

[22] T. A. Laplace *et al.*, Statistical properties of ^{243}Pu, and ^{242}Pu (n,γ) cross section calculation, Phys. Rev. C **93**, 014323 (2016).

[23] M. Guttormsen, T. E. Hansen, and N. Lietaer, The SiRi particle-telescope system, Nucl. Instrum. Meth. A **648**, 168 (2011).

[24] V. W. Ingeberg, F. Zeiser, and E. Lima, oslocyclotronlab/Qkinz: Update (Version 1.3.3). Zenodo (2018), http://doi.org/10.5281/zenodo.1206099.

[25] T. Tornyi, A. Görgen, M. Guttormsen, A. Larsen, S. Siem, A. Krasznahorkay, and L. Csige, A new fission-fragment detector to complement the CACTUS-SiRi setup at the Oslo Cyclotron Laboratory, Nucl. Instrum. Meth. A **738**, 6 (2014).

[26] F. Zeiser, G. Tveten, F. Bello Garrote, M. Guttormsen, A. Larsen, V. Ingeberg, A. Görgen, and S. Siem, The γ-ray energy response of the Oslo Scintillator Array OSCAR, Nucl. Instrum. Meth. A **985**, 164678 (2021).

[27] V. W. Ingeberg *et al.*, Characterization of the Oslo scintillator array OSCAR (unpublished).

[28] F. Zeiser, G. M. Tveten, F. L. Bello Garrote, M. Guttormsen, A. C. Larsen, V. W. Ingeberg, A. Görgen, and S. Siem, The energy response of the Oslo Scintillator Array OSCAR-Draft state Aug 2018, arXiv:2008.06240v1 [physics.ins-det] (2018) (draft version of Ref. [26]).

[29] F. Zeiser and G. M. Tveten, oslocyclotronlab/OCL_GEANT4: Geant4 model of OSCAR, OSCAR Response Function oscar2017scale1.15 (Version v1.0.3). Zenodo (2017), http://doi.org/10.5281/zenodo.1339347.

[30] M. Guttormsen, T. S. Tveter, L. Bergholt, F. Ingebretsen, and J. Rekstad, The unfolding of continuum y-ray spectra, Nucl. Instrum. Methods Phys. Res. A **374**, 371 (1996).

[31] J. E. Midtbø, F. Zeiser, E. Lima, A.-C. Larsen, G. M. Tveten, M. Guttormsen, F. L. Bello Garrote, A. Kvellestad, and T. Renstrøm, A new software implementation of the Oslo method with rigorous statistical uncertainty propagation, Comput. Phys. Commun. **262**, 107795 (2021).

[32] S. Bjørnholm and J. E. Lynn, The double-humped fission barrier, Rev. Mod. Phys. **52**, 725 (1980).

[33] V. V. Verbinski, H. Weber, and R. E. Sund, Prompt gamma rays from ^{235}U(n,f), ^{239}Pu(n,f), and spontaneous fission of ^{252}Cf, Phys. Rev. C **7**, 1173 (1973).

[34] R. Billnert, F.-J. Hambsch, A. Oberstedt, and S. Oberstedt, New prompt spectral γ-ray data from the reaction ^{252}Cf(sf) and its implication on present evaluated nuclear data files, Phys. Rev. C **87**, 024601 (2013).

[35] A. Oberstedt, R. Billnert, F.-J. Hambsch, and S. Oberstedt, Impact of low-energy photons on the characteristics of prompt fission γ-ray spectra, Phys. Rev. C **92**, 014618 (2015).

[36] A. Oberstedt, A. Gatera, A. Göök, and S. Oberstedt, Time response and its impact on prompt fission γ-ray spectra characteristics, Eur. Phys. J. A **56**, 196 (2020).

[37] R. Vogt, J. Randrup, D. A. Brown, M. A. Descalle, and W. E. Ormand, Event-by-event evaluation of the prompt fission neutron spectrum from ^{239}Pu(n,f), Phys. Rev. C **85**, 024608 (2012).

[38] R. Capote *et al.*, RIPL - reference input parameter library for calculation of nuclear reactions and nuclear data evaluations, Nucl. Data Sheets **110**, 3107 (2009).

[39] A. Oberstedt *et al.*, Improved values for the characteristics of prompt-fission γ-ray spectra from the reaction ^{235}U(n$_{th}$,f), Phys. Rev. C **87**, 051602(R) (2013).

[40] Data extracted from the ENDSF database using NNDC's Chart of Nuclides, https://www.nndc.bnl.gov/nudat2/.

[41] A. Oberstedt, R. Billnert, and S. Oberstedt, Predictions of characteristics of prompt-fission γ-ray spectra from the n + ^{238}U reaction up to E$_n$ = 20 MeV, Phys. Rev. C **96**, 034612 (2017).

[42] I. Stetcu, M. B. Chadwick, T. Kawano, P. Talou, R. Capote, and A. Trkov, Evaluation of the prompt fission gamma properties for neutron induced fission of ^{235,238}U and ^{239}Pu, Nucl. Data Sheets **163**, 261 (2020).

[43] H. Makii *et al.*, Effects of the nuclear structure of fission fragments on the high-energy prompt fission γ-ray spectrum in ^{235}U(n$_{th}$, f), Phys Rev C **100**, 044610 (2019).

[44] R. Vogt and J. Randrup, Angular momentum effects in fission, Phys. Rev. C **103**, 014610 (2021).

[45] P. Talou, I. Stetcu, P. Jaffke, M. E. Rising, A. E. Lovell, and T. Kawano, Fission fragment decay simulations with the CGMF code, arXiv:2011.10444v1.

[46] D. Gjestvang *et al.*, Zenodo repository for data in Fig. 6 from the article Excitation energy dependent prompt fission γ-ray emission from ^{241}Pu*, doi: 10.5281/zenodo.4333545 (2020).